

Goal-Conditioned Data Augmentation for Offline Reinforcement Learning

Xingshuai Huang, Di Wu *Member, IEEE*, and Benoit Boulet *Senior Member, IEEE*

Abstract—Offline reinforcement learning (RL) enables policy learning from pre-collected offline datasets, relaxing the need to interact directly with the environment. However, limited by the quality of offline datasets, it generally fails to learn well-qualified policies in suboptimal datasets. To address datasets with insufficient optimal demonstrations, we introduce *Goal-cOnditioned Data Augmentation (GODA)*, a novel goal-conditioned diffusion-based method for augmenting samples with higher quality. Leveraging recent advancements in generative modeling, GODA incorporates a novel return-oriented goal condition with various selection mechanisms. Specifically, we introduce a controllable scaling technique to provide enhanced return-based guidance during data sampling. GODA learns a comprehensive distribution representation of the original offline datasets while generating new data with selectively higher-return goals, thereby maximizing the utility of limited optimal demonstrations. Furthermore, we propose a novel adaptive gated conditioning method for processing noised inputs and conditions, enhancing the capture of goal-oriented guidance. We conduct experiments on the D4RL benchmark and real-world challenges, specifically traffic signal control (TSC) tasks, to demonstrate GODA’s effectiveness in enhancing data quality and superior performance compared to state-of-the-art data augmentation methods across various offline RL algorithms.

Index Terms—Offline reinforcement learning, diffusion model, data augmentation

I. INTRODUCTION

Reinforcement learning [1] aims to learn a control policy from trial and error through interacting with the environment. While demonstrating remarkable performance in various domains, this approach typically requires vast amounts of training data collected from these interactions. Such data-intensive requirements become impractical in applications where environmental interactions are costly, risky, or time-consuming, such as robotics [2], [3], autonomous driving [4], [5] and TSC [6], [7]. Offline RL offers a feasible solution to these challenges by enabling policy learning directly from pre-collected historical datasets, thus significantly reducing the need to interact directly with the environment.

Although offline RL makes policy learning less expensive, its performance is highly dependent on the quality of the pre-collected datasets and may suffer from lack of diversity, behavior policy bias, distributional shift, and suboptimal demonstrations [8]. The performance of offline RL tends to decline drastically when trained with suboptimal offline

datasets. Previous studies have attempted to address these issues by constraining the learned policy to align closely with the behavior policy [9] or by limiting out-of-distribution action values [10]. Although these approaches have shown performance improvements, they retain the inherent defects of offline datasets, remaining highly dependent on data quality.

Several studies have addressed the limitations of offline RL using data augmentation methods to generate more diverse samples. One approach involves learning world models to mimic environmental dynamics and iteratively generate synthetic rollouts from a start state [11], [12]. While this method significantly improves sample efficiency and data diversity, it suffers from compounding errors and fails to control the quality of generated trajectories. Other research leverages generative models to capture the distributions of collected datasets and randomly sample new transition data [13]. Although these methods demonstrate some performance improvements, they remain inefficient when dealing with datasets containing limited optimal demonstrations. This inefficiency stems from their inability to effectively control the quality of generated data.

We attempt to address this challenge by taking advantage of generative modeling to augment higher-quality data with directional goals. Unlike previous studies that sample data unconditionally and randomly [13], we introduce GODA to incorporate representative goals, guiding the samples toward higher returns. Given the exceptional performance of diffusion models [14], [15] in the field of generative artificial intelligence, GODA utilizes a diffusion model as its generative framework. GODA is trained to capture a comprehensive representation of the data distribution from the original dataset while sampling new data conditioned on selective high-return goals. This approach maximizes the utility of the limited well-performed trajectories in the original datasets.

Inspired by Decision Transformer [16], we define the ‘goal’ as the *return-to-go* (RTG), which represents the cumulative rewards from the current step until the end, coupled with its specific timestep in trajectories. RTG explicitly indicates the expected future rewards for a given behavior at the current timestep for a specific trajectory. We assume that at the same timestep across different trajectories, a higher RTG signifies a higher goal. To generate samples that exceed the quality of the original dataset, we introduce three *goal selection mechanisms* and a *scaling technique* to control our expected goals during sampling.

We present an illustrative example of how GODA operates in Figure 1. The task is to identify the shortest path from the starting point to the target. By setting higher RTG goals during

arXiv:2412.20519v1 [cs.LG] 29 Dec 2024

This work was supported by Fonds de recherche du Québec – Nature et technologies (FRQNT).

Xingshuai Huang, Di Wu, Benoit Boulet are with the Department of Electrical and Computer Engineering, McGill University; Email: xingshuai.huang@mail.mcgill.ca, di.wu5@mcgill.ca, benoit.boulet@mcgill.ca. Di Wu is the corresponding author.

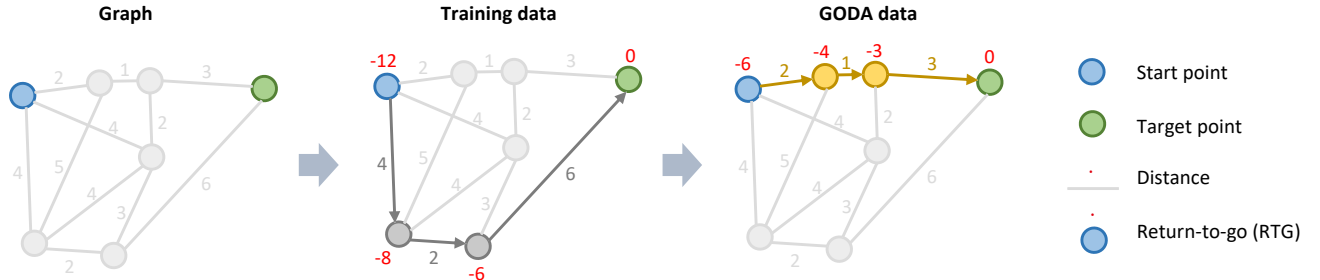


Fig. 1. Illustrative examples of how GODA augments higher-return data with goal guidance. GODA utilizes scalable RTG-based goal conditions to generate samples with higher returns (shorter overall distance).

sampling, GODA can potentially discover a more efficient route that yields a higher return (the RTG at the first timestep is equal to the return).

To better incorporate goal conditions, we further propose a novel *adaptive gated conditioning* approach. This method utilizes a condition-adaptive gated residual connection and an adaptive gated long skip connection to selectively capture multi-granularity information effectively with the guidance of goals. GODA is an off-the-shelf solution that can seamlessly integrate with other offline RL optimization approaches on various tasks to achieve superior results. We summarize our contributions:

1) We propose a goal-conditioned data augmentation method, namely GODA, for offline RL. It achieved enhanced data diversity and quality for offline datasets with limited optimal demonstrations.

2) We introduce novel *directional goals* with *selection mechanisms* and *controllable scaling* to provide higher-return guidance for the data sampling process in our employed generative models. Additionally, we propose a novel *adaptive gated conditioning approach* to better capture input information based on goal guidance.

3) We show GODA’s competence through comprehensive experiments on the *D4RL benchmark* compared with state-of-the-art data augmentation methods across multiple offline RL algorithms. We further evaluate the effectiveness of GODA on a real-world application, i.e., *traffic signal control* with small-size datasets obtained from widely used controllers in real-world deployments. These evaluations verify GODA’s effectiveness in addressing various challenges, significantly enhancing the applicability of RL-based methods for real-world scenarios.

The remaining sections are organized as follows: in Section II, we review recent researches on offline RL and data augmentation. Some preliminaries about offline RL and diffusion models are introduced in Section III, followed by details about our methodology in Section IV. Section V describes the experimental settings about D4RL and TSC tasks, baselines and evaluation algorithms. Next, we show the data quality measurement for our augmented datasets in Section VI and provide more detailed experimental results in Section VII. Finally, we conclude our research and discuss future directions in Section VIII.

II. RELATED WORK

A. Offline Reinforcement Learning

Offline RL involves learning policies from pre-collected offline datasets comprising trajectory rollouts generated by behavior policies. This approach is promising because it avoids the costs and risks associated with direct interactions with the environment. Conventional offline RL methods aim to alleviate the distributional shift problem, i.e., a significant drop in performance due to deviations between learned policy and the behavior policy used for generating the offline data [17]. To address this issue, various strategies have been employed, including explicit correction [18], such as constraining the policy to a restricted action space [19], and making conservative estimates of the value function [20], [21], with the aim of aligning the behavior policy with the learned policy.

Some recent studies exploit the strong sequence modeling ability of Transformer models to solve offline RL with trajectory optimization. For instance, Decision Transformer [16] and its variants [22], [23] utilize a GPT model to autoregressive predict actions given the recent subtrajectories composed of historical RTGs, states, and actions. These approaches integrate hindsight return information, i.e., RTG, with sequence modeling, eliminating the necessity for dynamic programming.

Diffusion models have also been adopted in offline RL given its exceptional capability of multi-modal distribution modeling. Diffuser [24] employs diffusion models for long-horizon planning, effectively bypassing the compounding errors associated with classical model-based RL. Hierarchical Diffuser [25] enhances this approach by introducing a hierarchical structure, specifically a jumpy planning method, to improve planning effectiveness further.

B. Data Augmentation in Offline Reinforcement Learning

Rather than passively reusing data and concentrating on enhancing learning algorithms, data augmentation proactively generates more diverse data to improve policy optimization. Some model-based RL methods employ learned world models from offline datasets to simulate the environment and iteratively generate synthetic trajectories, facilitating policy optimization [11]. For instance, TATU [11] uses world models to produce synthetic trajectories and truncates those with high accumulated uncertainty. However, model-based RL often suffers from compounding errors in the learned world models.

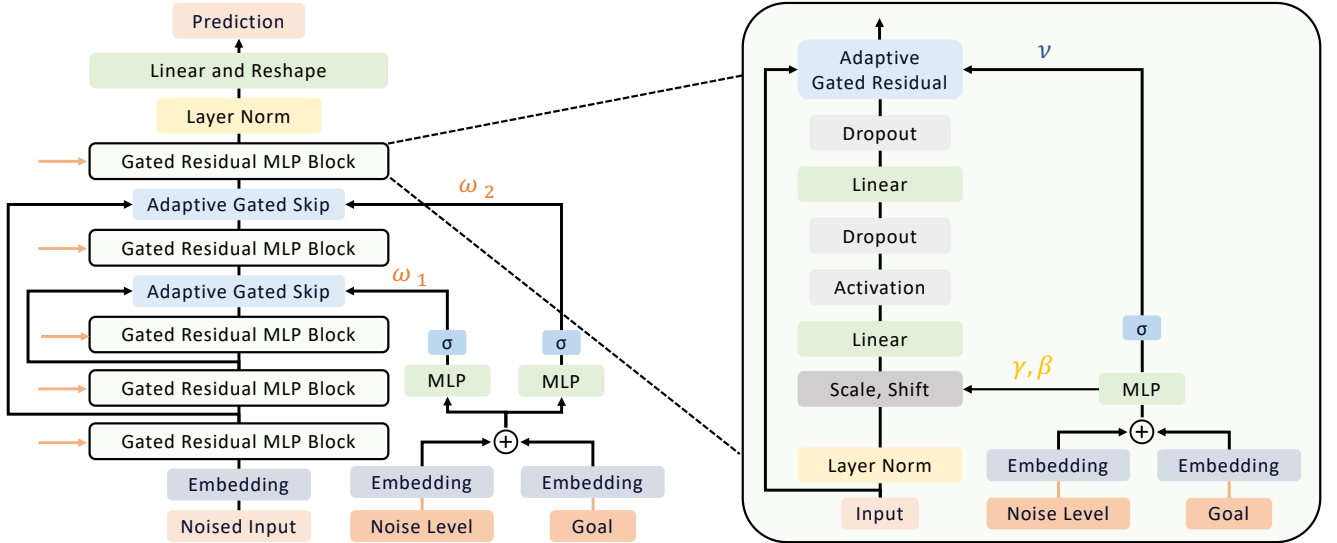


Fig. 2. The denoiser neural network with adaptive gated conditioning architecture. The *condition-adaptive gated long skip connection*, shown in the left part, captures both low- and high-level features, assigning varying importance weights to each. The *adaptive gated residual*, depicted in the right part, further enhances the model by selectively preserving input information based on the given conditions.

Some basic data augmentation functions (DAFs), i.e., translate, rotate, and reflect, are also applied to augment trajectory segments [26]. GuDA [27] further introduces human guidance into these DAFs to improve data quality, while human intervention is costly and lacks scalability. Diffusion models are also directly applied to data augmentation through the sampling process. SynthER [13] is the first work that employs diffusion models to learn the distribution of initial offline datasets and unconditionally augment large amounts of new random data. However, it fails to control the sampling process to steer toward high-return directions actively. DiffStitch [4] attempts to enhance the quality of generated data by actively connecting low-reward trajectories to high-reward ones using a stitching technique.

We propose enhancing the quality of generated data from a different perspective by introducing a controllable directional goal into our generative modeling. This approach selectively reuses optimal trajectories to guide the sampling process toward achieving higher returns.

III. PRELIMINARIES

A. Offline Reinforcement Learning

In RL, the task environment is generally formulated as a Markov decision process (MDP) $\{\mathcal{S}, \mathcal{A}, \mathcal{R}, \mathcal{P}, \gamma\}$ [1]. $s \in \mathcal{S}$, $s' \in \mathcal{S}$, $a \in \mathcal{A}$, $r = \mathcal{R}(s, a)$, $\mathcal{P}(s'|s, a)$, and $\gamma \in [0, 1)$ represent state, next state, action, reward function, state transition, and discount factor, respectively. RL aims to train an agent to interact with the environment and learn a policy π from experience. The objective of RL is to maximize the expected discounted cumulative rewards over time:

$$J = \mathbb{E}_{\pi} \left[\sum_{t=0}^{\infty} \gamma^t \mathcal{R}(s_t, a_t) \right], \quad (1)$$

where t denotes the timestep in a trajectory. For offline RL, the policy is learned directly from offline datasets pre-

collected by other behavior policies, instead of environmental interactions. The offline dataset typically consists of historical experience described as tuples (s, a, r, s') and other environmental signals. After learning a policy $\pi(\mathcal{D})$ from dataset \mathcal{D} , the performance is evaluated in online environment as $\mathbb{E}_{\pi(\mathcal{D})} \left[\sum_{t=0}^{\infty} \gamma^t \mathcal{R}(s_t, a_t) \right]$.

While offline RL eliminates reliance on interacting with the environment, it is highly restricted by the quality of offline datasets due to the lack of feedback from the environment. Our GODA aims to enhance the diversity and quality of the dataset by upsampling the pre-collected data to an augmented dataset \mathcal{D}^* . The objective is to learn a policy $\pi(\mathcal{D}^*)$ that outperform $\pi(\mathcal{D})$ learned from original dataset \mathcal{D} , such that

$$\mathbb{E}_{\pi(\mathcal{D}^*)} \left[\sum_{t=0}^{\infty} \gamma^t \mathcal{R}(s_t, a_t) \right] > \mathbb{E}_{\pi(\mathcal{D})} \left[\sum_{t=0}^{\infty} \gamma^t \mathcal{R}(s_t, a_t) \right]. \quad (2)$$

B. Diffusion Models

Diffusion models [28], [14], [15], a class of well-known generative modeling methods, aim to learn a comprehensive representation of the data distribution $p_{\text{data}}(\mathbf{x}^N)$ with a standard deviation σ_{data} from a given dataset. Diffusion models generally have two primary processes, the *forward process*, also known as the *diffusion process*, and the *reverse/sampling process*.

The forward process is characterized by a Markov chain in which the original data distribution $\mathbf{x}^N \in p_{\text{data}}(\mathbf{x}^N)$ is progressively perturbed with a predefined i.i.d. Gaussian noise schedule $\sigma^N = 0 < \sigma^{N-1} < \dots < \sigma^0 = \sigma_{\text{max}}$. Therefore, we can obtain a sequence of noised distributions $p(\mathbf{x}^i; \sigma^i)$ for each noise level σ^i , where the last noised distribution $p(\mathbf{x}^0; \sigma_{\text{max}})$ can be seen as pure Gaussian noise when $\sigma_{\text{max}} \gg \sigma_{\text{data}}$.

For reverse process, Denoising Diffusion Probabilistic Model (DDPM) [14] models it as a Markov chain that involves denoising an initial noise $p(\mathbf{x}^0) = \mathcal{N}(\mathbf{x}^0; \mathbf{0}, \mathbf{I})$ to the original

data distribution with learned Gaussian transitions. Elucidated Diffusion Model (EDM) [15] formulates the forward and reverse processes as a probability-flow ODE, where the noise level can be increased or decreased by moving the ODE forward or backward in time:

$$d\mathbf{x} = -\dot{\sigma}(t_i)\sigma(t_i)\nabla_{\mathbf{x}}\log p(\mathbf{x};\sigma(t_i))dt_i, \quad (3)$$

where $\dot{\sigma}(t_i)$ denotes derivative over denoise time and $\nabla_{\mathbf{x}}\log p(\mathbf{x};\sigma(t_i))$ is referred to as the score function [29], which points towards regions of higher data density. It is worth noting that we use t_i to denote the noise time to distinguish it from the trajectory timestep t . The ODE pushes the samples away from the data or closer to the data through infinitesimal forward or backward steps. The corresponding step sequence is $\{t_0, t_1, \dots, t_N\}$, where $t_N = 0$ and N denotes the number of ODE solver iterations.

EDM proposes to estimate the score function using denoising score matching [15]. Specifically, a denoiser neural network $D_{\theta}(\mathbf{x};\sigma)$ is trained to approximate data \mathbf{x}^N sampled from p_{data} by minimizing the L_2 denoising loss independently for each σ :

$$\min_{\theta} \mathbb{E}_{\mathbf{x}^N \sim p_{\text{data}}; \mathbf{n} \sim \mathcal{N}(\mathbf{0}, \sigma^2 \mathbf{I})} \|D_{\theta}(\mathbf{x}^N + \mathbf{n}; \sigma) - \mathbf{x}^N\|_2^2. \quad (4)$$

Subsequently, the score function can be calculated as $\nabla_{\mathbf{x}}\log p(\mathbf{x};\sigma) = (D_{\theta}(\mathbf{x};\sigma) - \mathbf{x})/\sigma^2$.

IV. METHODOLOGY

In this section, we introduce GODA, a goal-conditioned data augmentation method utilizing generative modeling for augmenting higher-quality synthetic transition data. Our adopted diffusion model learns comprehensive data distribution from the initial offline dataset, subsequently sampling new data towards higher return with controllable selective goal conditions. In this part, we define a representative goal for GODA and introduce different selective mechanisms for goal conditions. To proactively control the sampling direction, a controllable goal scaling factor is introduced. For better integrating goal conditions as guidance within the diffusion model, we further propose a novel adaptive gated conditioning approach that introduces condition-adaptive gate mechanism into long skip connection and residual connection.

A. Return-oriented goal

Prior diffusion-based work [13] lacks the ability to guide the sampling process in the desired direction. We attempt to introduce a return-oriented goal as a condition of our diffusion model. Inspired by Decision Transformer, we adopt RTG [16], cumulative rewards from the current step till the end, as the explicit goal condition

$$\hat{g}_t = \sum_{t'=t}^T r_{t'}. \quad (5)$$

For each transition sample represented as a tuple (s, a, s', r) within a trajectory, RTG quantifies the expected future rewards for the current behavior, effectively serving as a goal. In other words, a higher RTG at a specific timestep typically

Algorithm 1 GODA: Goal-Conditioned Data Augmentation

- 1: Initialize generative model G_{θ} and $\mathcal{D}^* = \emptyset$
 - 2: Split initial offline dataset \mathcal{D} into trajectories according to episode terminal information
 - 3: Calculate RTGs for each transition sample in trajectories
 - 4: Add RTGs and timesteps as goals into \mathcal{D}
 - 5: Train G_{θ} on \mathcal{D} using Eq. 9 by conditioning on goals
 - 6: **repeat**
 - 7: Extract goal conditions for sampling according to the goal selection mechanism.
 - 8: Re-assign sampling goal conditions with goal scaling factor λ using Eq. 6
 - 9: Sampling a batch of new transition samples \mathcal{B}^*
 - 10: $\mathcal{D}^* \leftarrow \mathcal{D}^* \cup \mathcal{B}^*$
 - 11: **until** end
 - 12: Train policy π on the final dataset $\mathcal{D}^* \cup \mathcal{D}$
-

signifies a higher goal for the policy to pursue. Since the same behavior at different timesteps often yields varying RTGs across different trajectories, we combine the RTG with its corresponding timestep in the trajectory as the condition for each specific transition sample. The timestep signal acts as a timestamp for each goal.

B. Selective goal conditions

During dataset preprocessing, we first organize offline samples into trajectories, compute the RTG for each, and append timesteps to every sample. To fully leverage well-performing samples and augment samples with higher returns, we propose three distinct condition selection mechanisms: return-prior, RTG-prior, and random goal conditions.

(1) Return-prior goal condition. In this approach, we rank all trajectories based on their return values and select the top n trajectories. During the sampling process of the diffusion model, the RTG and timestep pairs (\hat{g}_t, t) from these top n trajectories are selected as the sampling goal conditions. This method filters high-return trajectories from the initial offline datasets and reuses them to sample more well-optimized transitions.

(2) RTG-prior goal condition. We group RTGs by their associated timesteps and then sort them to select the top n RTGs along with their corresponding timesteps as goal conditions. This approach selectively reuses high-RTG transitions for data augmentation, focusing on transitions that are most likely to yield higher returns.

(3) Random goal condition. We randomly select m RTG and timestep pairs (\hat{g}_t, t) as sampling goal conditions for each batch of samples. This increases the diversity of the augmented data while paying less attention to the optimal trajectories for improving performance.

C. Controllable goal scaling

Selective goal conditions offer high-return guidance during the sampling process but are limited in generating data with returns or quality beyond the initial offline datasets. To overcome this limitation, we introduce a controllable goal scaling factor,

λ , which can be multiplied with the goal values to represent a higher return expectation. This approach enables flexible adjustment of goal values to drive the sampling process toward higher-quality data. As illustrated in Figure 1, a higher RTG goal at each timestep directs the sampling process toward a trajectory with a greater overall return. Figure 3 depicts that higher goals guide the sampling process towards higher-reward data regions. Since RTG values can be either positive or negative in certain tasks, we propose multiplying positive goals by the scaling factor and dividing negative goals by it.

$$\text{goal} = \begin{cases} (\lambda \hat{g}_t, t), & \hat{g}_t \geq 0 \\ (\hat{g}_t / \lambda, t), & \hat{g}_t < 0. \end{cases} \quad (6)$$

It is worth noting that a goal increment factor is not applicable to RTG-based goals, since incrementing all RTGs for a trajectory simply means only incrementing the reward at first timestep while keeping all remaining rewards unchanged.

D. Adaptive Gated Conditioning

To better capture goal guidance and seamlessly integrate conditions into the diffusion model, we propose a novel adaptive gated conditioning approach, as shown in Figure 2. This structure significantly enhances the ability to guide the diffusion and sampling processes using goal conditions. The conditional inputs include both the noise level condition and goal condition, which are embedded separately, then element-wise added, and fed into the neural network. The noise input is processed with several gated residual multi-layer perception (MLP) blocks with novel adaptive gated skip connections between shallow and deep layers.

1) *Condition Embedding*: The noise level σ for diffusion is encoded using Random Fourier Feature [30] embedding. The RTG is processed with a linear transformation to get a hidden representation. The timestep of each RTG is embedded with Sinusoidal positional embedding [31]. We concatenate the RTG and timestep embeddings to form the goal condition, which is then element-wise added to the noise level embedding and used as the conditional input.

2) *Adaptive Gated Long Skip Connection*: As shown in the left part of Figure 2, we adopt a long skip connection similar to U-Net [32] to connect MLP blocks at different levels. To capture different information with varying importance weights, we propose a novel adaptive gated long skip connection structure by adding the previous information with an adaptive gate mechanism based on the given conditions.

$$x_{\text{out}} = (1 - \omega) * x_{\text{skip}} + \omega * x, \quad (7)$$

where x_{skip} and x are outputs of a shallower and the previous block, and ω denotes a learnable weight calculated by regressing the conditional input with an MLP and a sigmoid layer.

3) *Gated Residual MLP Block*: The right part of Figure 2 depicts the structure of each gated residual MLP block. We adopt the widely used adaptive layer normalization (adaLN) method [33] to learn dimension-wise scale γ and shift β based on the conditional information. Besides, we explore a modification of the residual connection [34] and introduce a

TABLE I
HYPERPARAMETER SETTINGS FOR DENOISER NETWORK.

Hyperparameter	Value
embedding dimension	128
MLP width	512
MLP activation	SiLU
gate activation	Sigmoid
learning rate	0.0003
batch size	256
learning rate schedule	cosine annealing
optimizer	Adam
gradient update steps	100K

TABLE II
HYPERPARAMETER SETTINGS FOR THE DIFFUSION MODEL.

Hyperparameter	Value
number of diffusion steps	128
S_{churn}	80
S_{tmin}	0.05
S_{tmax}	50
S_{noise}	1.003
σ_{min}	0.002
σ_{max}	80

novel condition-adaptive gated residual connection to further enhance the model by selectively preserving input information. It also regresses the conditional input and gets a learnable weight ν for adaptively preserving input information.

$$x_{\text{out}} = (1 - \nu) * F(x) + \nu * x, \quad (8)$$

where F is the learned transformation.

E. Model Implementation

Given the strong ability of diffusion models to capture complex data distribution and generate high-dimension data, we adopt EDM [15] as our generative model for augmenting offline data. The neural network equipped with adaptive gated conditioning as illustrated in Figure 2 is used as the denoiser function. We train the generative model to approximate the data distribution of the offline dataset and use every transition tuple as a training sample. Given the non-sequence input format, we do not consider complicated structures, e.g., attention mechanisms, but use simple MLPs to process inputs. Algorithm 1 shows the learning process of our GODA method. With goal conditions \mathbf{c} and transition data \mathbf{x} from the original datasets, the generative model G_θ with a learnable denoiser neural network D_θ is trained by

$$\min_{\theta} \mathbb{E}_{\mathbf{x}, \mathbf{c} \sim p_{\text{data}}; \mathbf{n} \sim \mathcal{N}(\mathbf{0}, \sigma^2 \mathbf{I})} \|D_\theta(\mathbf{x} + \mathbf{n}; \sigma; \mathbf{c}) - \mathbf{x}\|_2^2. \quad (9)$$

After obtaining a well-trained conditional diffusion model, we leverage it for sampling data and store data in augmentation dataset \mathcal{D}^* for further policy training.

F. Hyperparameters

We show more details about the hyperparameter settings of the GODA model.

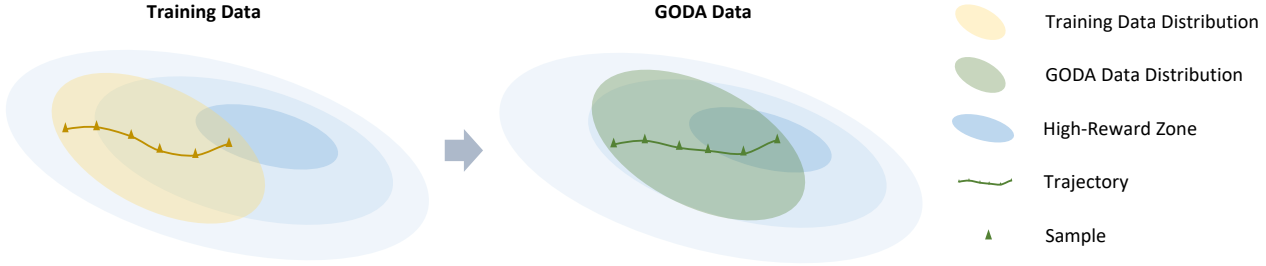


Fig. 3. An illustrative example of how GODA utilizes higher goals to steer the sampling process toward higher-reward data distribution region.

1) *Denoising Network*: The denoising neural network utilizes the adaptive gated conditioning architecture, as shown in Figure 2. Table I details the associated hyperparameters. We use Random Fourier Feature embedding [30] and Sinusoidal positional embedding [31] to process the noise level and timestep of each RTG respectively, with an embedding dimension of 128. The width of the linear layers in the MLP block is set to 512, with SiLU [35] as the activation function. The total number of trainable parameters for the denoiser neural network is approximately 3.3M. We train our GODA model with 100K steps of gradient updates, with a batch size of 256 and a learning rate of 0.0003.

2) *Elucidated Diffusion Model*: We adopt EDM [15] as our diffusion model and follow the original settings from SynthER [13], with the default hyperparameters shown in Table II. EDM employs Heun’s 2nd order ODE solver [36] to solve the reverse-time ODE, enabling data sampling through the reverse process. The diffusion timestep is set to 128 for higher-quality results. All training and sampling are conducted on an AMD Ryzen 7 7700X 8-Core Processor and a single NVIDIA GeForce RTX 4080 GPU. Training GODA for 100K steps takes approximately 14 minutes while generating 5M samples with a sampling batch size of 250K requires about 300 seconds.

V. EXPERIMENTAL SETTINGS

In this section, we provide a comprehensive overview of the experiments conducted to evaluate the performance of our proposed GODA method.

A. D4RL Tasks and Datasets.

We adopt three popular Mujoco locomotion tasks from Gym¹, i.e., HalfCheetah, Hopper, and Walker2D, and a navigation task, i.e., Maze2D [37], as well as more complex tasks, specifically the Pen and Door tasks from the Adroit benchmark [38], [37].

1) *Gym*: In the case of Gym tasks where dense rewards are available, we employ three distinct data configurations from the D4RL datasets: Random, Medium-Replay, and Medium. To elaborate, Random datasets contain transition data generated by a randomly initialized policy. Medium datasets consist of a million data points gathered using a policy that achieves

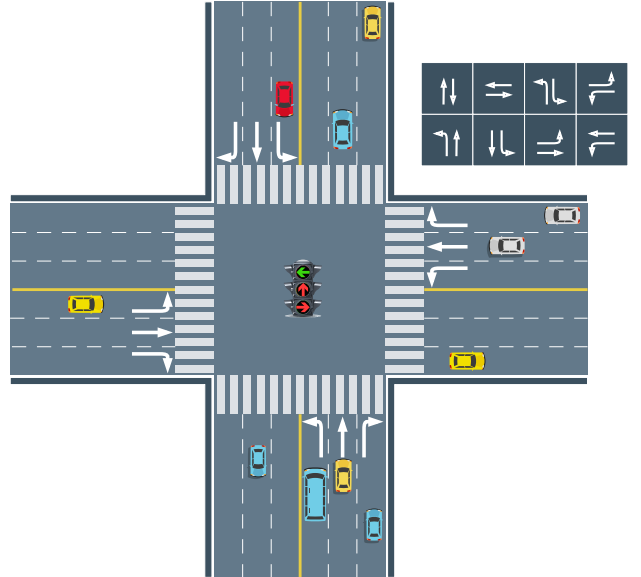


Fig. 4. A standard signalized intersection with four three-lane approaches and eight phases.

one-third of the performance of an expert approach. Medium-replay datasets contain the stored experience in a replay buffer during the training of a policy until it reaches the score in Medium datasets.

2) *Maze2D*: For Maze2D, a 2D agent is trained to reach a goal position utilizing minimal feedback i.e., a single point for success, zero otherwise. Three datasets collected from different maze layouts are adopted, i.e., Umaze, Medium, and Large.

3) *Adroit*: Besides, we further test our GODA on more complex tasks, specifically the Pen and Door tasks from the Adroit benchmark [38], [37]. These tasks involve manipulating a pen and opening a door using a 24-DoF simulated hand robot. For each task, we use two different datasets: Human and Cloned. The Human dataset consists of trajectories from human demonstrations, while the Cloned dataset is generated by applying an imitation policy trained from a mix of human and expert demonstrations and combining the resulting trajectories with the demonstrations in a 50/50 split.

B. Traffic Signal Control Tasks and Datasets.

To evaluate GODA’s applicability to real-world challenges, we further test it on TSC tasks with much fewer training

¹<https://www.gymlibrary.dev/environments/mujoco/>

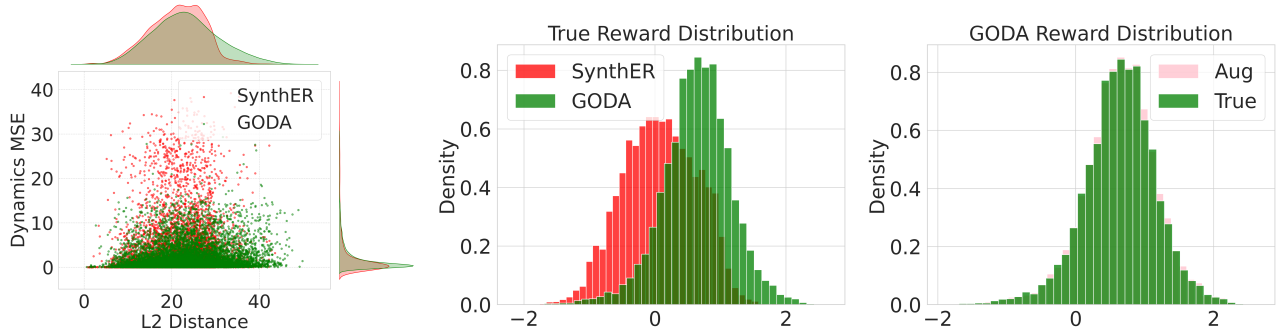


Fig. 5. Data quality evaluation for SynthER and GODA on Walker2D-Random-V2. **Left:** Dynamics MSE and L2 Distance comparison. Smaller Dynamics MSE indicates better validity and larger L2 Distance indicates higher diversity. **Middle:** Ground-truth reward distributions from the simulator for augmented datasets. **Right:** Ground-truth and augmented reward distributions for GODA dataset.

TABLE III
DATA QUALITY EVALUATION METRICS FOR SYNTHER AND GODA ON WALKER2D TASKS. SMALLER DYNAMICS MSE, LARGER L2 DISTANCE, AND LARGER AVERAGE REWARD INDICATE BETTER QUALITY.

Task	Dynamics MSE		L2 Distance		Average Reward	
	SynthER	GODA	SynthER	GODA	SynthER	GODA
Walker2D-Random-v2	2.7±5.7	1.9±2.9	21.8±7.0	23.2±7.6	0.1±0.6	0.6±0.5
Walker2D-Medium-Replay-v2	0.5±1.7	0.4±1.1	17.3±6.3	17.2±6.0	2.5±1.3	3.5±0.9
Walker2D-Medium-v2	0.3±1.0	0.3±0.8	11.7±5.2	11.8±5.3	3.4±1.2	3.7±0.9

samples using the CityFlow simulator [39]. TSC aims to optimize traffic flow by efficiently managing traffic signals to maximize overall traffic efficiency. As shown in Figure 4, a signalized intersection in TSC problems is composed of approaches with several lanes in each approach. The controller manages the phase as shown in the top right part of Figure 4, which determines the activated traffic signals for different directions, to control the orderly movement of vehicles.

To evaluate our GODA, we select three real-world scenarios featuring a 12-intersection grid from Jinan (JN) city and two scenarios with a 16-intersection grid from Hangzhou (HZ) city [6]. These scenarios represent a variety of traffic patterns and intersection structures, allowing us to cover a wide range of traffic situations. To bridge the gap between simulation and real-world conditions, we use the widely adopted Fixed-Time (FT) controller as one of our behavior policies for generating the initial offline datasets. Additionally, we employ Advanced Max Pressure (AMP) [40] and Advanced CoLight (ACL) [40] to create higher-quality datasets for further evaluation.

C. Baseline Methods

To verify the effectiveness of our proposed GODA, we compare it with three state-of-the-art data augmentation methods:

TATU² [11], which learns world models to generate synthetic rollouts and truncates trajectories with high accumulated uncertainty.

SynthER³ [13], which employs diffusion models to unconditionally augment large amounts of new data based on the learned distribution of original datasets.

DiffStitch⁴ [4], which augments data with a diffusion model and three MLPs, and actively connects low to high-reward trajectories with stitch techniques.

D. Evaluation Algorithms

To verify the quality of datasets augmented by GODA, we follow the evaluation settings adopted in previous data augmentation studies. We train two widely-used offline RL algorithms, i.e., IQL [10] and TD3+BC [41], on datasets and evaluate the learned policy on D4RL tasks. For TSC tasks, we utilize BCQ [42], CQL [21], and DataLight [6] as the evaluation algorithms.

It is important to note that for GODA, we train the evaluation algorithms using a mix of the original datasets and the augmented datasets, whereas for the other baseline methods, only the augmented datasets are used. This is because GODA focuses on augmenting samples from the high-reward zones, which may lead to reduced data diversity. In contrast, the baseline methods, as reported in their respective papers [13] and our experiments, exhibit degraded or similar performance when using a mix of the original and augmented datasets, as illustrated in Section VII-C5.

E. Implementation Details

1) *D4RL Tasks:* We augment 5M samples for each D4RL task. For the sampling process, we use the return-prior goal condition selection method and set the goal scaling factor to 1.1 for all tasks. We use the implementation of IQL and TD3+BC from the Clean Offline Reinforcement Learning (CORL) codebase [43] for D4RL tasks.

²<https://github.com/pipixiaqishi1/TATU>

³<https://github.com/conglu1997/SynthER>

⁴<https://github.com/guangheli2/DiffStitch>

TABLE IV

NORMALIZED SCORES OF GODA AND BASELINE DATA AUGMENTATION METHODS. THE RESULTS ARE CALCULATED ACROSS 5 RANDOM SEEDS. VALUES IN BOLD REPRESENT THE BEST PERFORMANCE (LARGEST SCORE).

Task	Dataset	IQL				TD3+BC					
		Original	TATU	SynthER	DStitch	GODA	Original	TATU	SynthER	DStitch	GODA
Halfcheetah	Rand	15.2±1.2	17.7±2.9	17.2±3.4	15.8±2.0	19.5±0.5	11.3±0.8	12.1±2.3	12.2±1.1	11.8±1.4	12.5±1.3
	Med-R	43.5±0.4	44.2±0.1	46.6±0.2	44.7±0.1	47.5±0.4	44.8±0.7	44.5±0.3	45.9±0.9	44.7±0.3	44.9±0.2
	Med	48.3±0.1	48.2±0.1	49.6±0.3	49.4±0.1	50.4±0.1	48.1±0.2	48.1±0.2	49.9±1.2	50.4±0.5	48.5±0.1
Walker2D	Rand	4.1±0.8	6.3±0.5	4.2±0.3	4.6±1.1	14.3±7.1	0.6±0.3	6.5±4.3	2.3±1.9	2.4±1.0	4.2±1.8
	Med-R	82.6±8.0	75.0±12.1	83.3±5.9	86.6±2.8	96.1±4.9	85.6±4.6	62.1±10.4	90.5±4.3	89.7±4.2	93.0±5.6
	Med	84.0±5.4	76.6±10.7	84.7±5.5	83.2±2.2	79.1±2.4	82.7±5.5	75.8±3.5	84.8±1.4	83.4±1.7	86.2±0.7
Hopper	Rand	7.2±0.2	8.1±2.9	7.7±0.1	6.5±0.9	8.7±2.1	8.6±0.3	18.1±11.5	14.6±9.4	8.8±2.3	8.2±0.1
	Med-R	84.6±13.5	79.6±7.6	103.2±0.4	102.1±0.4	102.5±0.6	64.4±24.8	64.1±10.5	53.4±15.5	79.6±13.5	63.0±12.8
	Med	62.8±6.0	60.3±3.6	72.0±4.5	71.0±4.2	74.3±2.9	60.4±4.0	58.3±4.8	63.4±4.2	60.3±4.9	74.8±3.6
Average	48.0±4.4	46.2±4.3	52.1±2.4	51.5±1.5	54.7±2.2	45.2±7.4	43.3±4.2	46.3±4.7	47.9±3.3	48.4±3.9	
Maze2D	Umaze	37.7±2.0	33.0±4.8	41.0±0.7	38.5±6.2	59.5±2.6	29.4±14.2	37.7±10.9	37.6±14.4	38.4±7.5	46.4±8.3
	Med	35.5±1.0	35.1±1.3	35.1±2.6	35.5±1.5	35.8±2.6	59.5±41.9	73.8±36.9	65.2±36.1	66.8±30.9	86.5±26.4
	Large	49.6±22.0	69.1±20.1	60.8±5.3	68.4±12.6	109±16.5	97.1±29.3	93.1±25.3	92.5±38.5	92.4±36.2	104.3±20.1
Average	40.9±8.3	45.7±8.2	45.6±2.9	47.5±6.8	68.1±6.6	62.0±28.2	68.2±10.6	65.1±29.7	65.9±24.9	79.1±7.5	

TABLE V

NORMALIZED SCORES OF GODA AND BASELINE DATA AUGMENTATION METHODS ON ADROIT TASKS EVALUATED USING IQL.

Task	Dataset	Original	TATU	SynthER	DStitch	GODA
Pen	Human	79.1±28.5	88.9±22.6	96.8±8.6	87.4±8.6	75.6±31.4
	Cloned	45.8±29.9	52.5±27.9	45.3±23.4	64.0±29.6	64.8±20.6
	Average	62.4±29.2	70.7±25.2	71.0±16.0	75.7±19.1	70.2±26.0
Door	Human	1.6±2.1	7.0±1.6	8.3±2.2	10.0±2.5	14.8±5.0
	Cloned	-0.1±0.5	-0.1±0.3	5.9±1.8	4.4±0.4	16.8±6.1
	Average	0.8±1.3	3.5±1.0	7.1±2.0	7.2±1.4	15.8±5.5

2) *TSC Tasks*: We formulate the TSC problem as a MDP and define the state, action, and reward function as follows:

State. For behavior policies (AMP and ACL), the state representation includes the current phase, traffic movement efficiency pressure, and the number of effective running vehicles [40]. For evaluation algorithms, BCQ and CQL use the same state representation as AMP, while DataLight adopts the number of vehicles, along with the total velocity saturation and unsaturation degrees [6].

Action. The action is generally defined as the phase selection for the next time period.

Reward. AMP, BCQ, CQL and DataLight use pressure [40] as the reward while ACL uses queue length. It is worth noting that we use the opposite of these metrics as the final reward function.

Due to the absence of certain key signals in the original datasets from the DataLight codebase, we generate a total of 24K samples for each dataset using the behavior policies for each task. Additionally, we augment 20K samples for each task using our GODA model. The task horizon for each TSC scenario is set to 3600 seconds, with a control step of 15 seconds. For the sampling process, we employ the return-prior goal condition selection method and set the goal scaling factor to 1.2 in TSC tasks. For evaluation methods, we employ the implementation of BCQ, CQL, and DataLight from <https://github.com/LiangZhang1996/DataLight>.

VI. AUGMENTED DATA QUALITY MEASUREMENT

Since our GODA is built upon SynthER, we compare the quality of the datasets augmented by both SynthER and GODA

to assess whether the goal conditions incorporated by GODA enhance data quality. We adopt two metrics from SynthER [13]:

$$\text{Dynamics MSE} = \frac{1}{M} \sum_{i=1}^M ((s_{t+1}^i, r_t^i) - (\hat{s}_{t+1}^i, \hat{r}_t^i))^2, \quad (10)$$

$$\text{L2 Distance} = \|(s_t^i, a_t^i) - (\bar{s}_t^i, \bar{a}_t^i)\|_2, \quad (11)$$

and introduce an Average Reward for evaluating reward distributions of augmented datasets

$$\text{Average Reward} = \frac{1}{M} \sum_{i=1}^M \hat{r}_t^i, \quad (12)$$

where M is the selected number of samples, $s_t^i, a_t^i, s_{t+1}^i, r_t^i$ denote the samples from augmented datasets, \hat{s}_{t+1}^i and \hat{r}_t^i denote the next state and reward generated by the simulator given states and actions from augmented datasets, and \bar{s}_t^i and \bar{a}_t^i are the state and action from original datasets.

Dynamics MSE measures how well the augmentation models capture the dynamics of the environment by learning patterns from the original datasets and generating data that aligns with those dynamics. L2 Distance assesses the models' exploration capabilities and data diversity by calculating the Euclidean distance between the augmented dataset and the original dataset, reflecting how diverse the generated data is. Average Reward compares the ground-truth reward distributions produced by the simulator given states and actions in datasets augmented by SynthER and GODA.

The left part of Figure 5 presents a scatter plot of 10K points sampled from the augmented datasets. Results show that

TABLE VI
AVERAGE TRAVEL TIME COMPARISON ON REAL-WORLD TSC TASKS. **SMALLER** TRAVEL TIME INDICATES BETTER TRAFFIC EFFICIENCY.

Traffic	Dataset	BCQ			CQL			DataLight		
		Original	SynthER	GODA	Original	SynthER	GODA	Original	SynthER	GODA
JN 1	FT	269.7±4.1	267.9±2.7	264.1±4.4	272.0±2.1	273.4±2.5	271.7±4.5	279.8±2.9	274.1±1.6	270.7±4.1
	AMP	271.5±3.9	264.0±6.1	259.7±0.9	261.8±0.3	261.7±4.3	260.6±3.4	298.1±3.1	299.2±2.0	301.7±1.4
	ACL	271.1±2.4	271.9±1.4	270.6±0.3	273.3±1.6	275.2±4.4	273.2±4.3	256.4±3.2	258.4±2.5	255.3±0.3
JN 2	FT	267.2±3.6	265.5±1.2	266.6±5.1	269.3±0.3	275.3±6.9	272.5±1.9	293.9±1.7	288.2±2.2	281.0±0.3
	AMP	250.7±0.7	254.7±2.6	252.1±3.4	251.9±4.0	249.4±5.3	245.5±1.0	244.4±2.3	240.0±2.2	240.9±4.0
	ACL	253.4±0.3	265.7±1.5	262.0±4.5	248.1±0.3	248.2±2.1	248.0±2.0	241.9±0.3	236.4±0.3	235.1±0.5
JN 3	FT	266.9±3.6	263.5±4.9	257.3±3.4	268.0±0.7	273.7±2.3	267.1±2.8	302.6±1.9	299.9±5.0	299.8±1.8
	AMP	263.8±3.1	259.3±0.7	253.2±4.4	251.5±2.9	247.7±4.9	242.5±3.5	239.4±1.8	241.8±4.9	232.5±1.7
	ACL	242.2±4.0	245.7±0.6	243.2±1.6	242.1±1.4	244.5±4.0	245.5±7.1	240.3±3.6	234.7±1.3	230.1±2.7
Average		267.9±3.2	267.1±2.3	263.9±2.7	264.8±1.9	265.7±4.2	262.4±3.2	267.5±2.1	265.5±2.3	262.6±1.4
HZ 1	FT	324.5±7.3	313.2±2.0	310.5±0.8	317.4±5.7	315.5±4.0	307.1±2.7	290.1±0.6	290.8±0.3	287.2±0.3
	AMP	295.8±4.6	302.7±1.9	301.7±4.1	300.0±0.3	295.1±0.3	285.4±1.0	287.3±4.3	284.9±3.8	286.1±3.2
	ACL	281.7±1.1	281.3±6.5	281.1±1.3	288.6±3.3	286.3±2.8	278.9±2.1	284.9±5.6	282.1±1.7	278.0±3.8
HZ 2	FT	340.0±4.9	340.7±4.6	341.3±1.5	341.7±2.7	334.8±1.4	331.6±1.9	308.0±0.3	308.4±3.1	309.2±3.0
	AMP	332.5±0.3	324.8±3.0	316.9±1.9	318.0±0.6	321.9±3.3	321.4±3.7	312.3±3.6	310.4±2.2	308.4±2.2
	ACL	336.7±1.9	329.3±0.5	327.1±2.8	347.4±3.8	343.9±2.6	336.8±0.3	317.6±4.1	314.8±4.1	315.4±3.0
Average		317.3±2.6	315.8±3.3	313.6±2.3	319.1±2.1	316.4±2.1	310.8±1.8	302.0±3.6	300.1±3.0	299.4±3.0

datasets generated by GODA exhibit much lower Dynamics MSE and a wider range of L2 Distance values, indicating both better alignment with environmental dynamics and greater diversity. The superior validity in performance may stem from the goal conditions (RTG-timestep pairs), which provide critical information for generating samples that better match the environment’s dynamics. Meanwhile, the increased diversity is likely due to the scaled out-of-distribution goal conditions incorporated in the sampling process.

The middle part demonstrates that GODA not only generates samples within a high-reward data zone but also extends the boundary of high rewards beyond the best demonstrations, compared to SynthER. The right part shows that the rewards generated by GODA align closely with the ground-truth values.

The evaluation results for the three metrics in Table III further demonstrate that GODA outperforms SynthER in terms of all data quality evaluation metrics across nearly all Walker2D tasks.

VII. EXPERIMENTAL RESULTS

A. Performance on D4RL

1) *Gym tasks.*: Table 1 presents a performance comparison between GODA and other state-of-the-art data augmentation methods trained on the D4RL Gym and Maze2D. We adopt the results of Original and SynthER from the SynthER paper [13], and those of TATU and DStitch from the DStitch [4] paper. We further conduct experiments for tasks not covered in the literature. As shown in the results, GODA consistently outperforms other methods across most Gym locomotion tasks when evaluated with both IQL and TD3+BC, resulting in higher average scores. Notably, even for tasks using Random datasets, GODA successfully leverages limited high-quality samples to enhance data quality, leading to improved final performance.

2) *Maze2D tasks.*: For Maze2D tasks where rewards are sparse, GODA demonstrates significant improvements across

all datasets, achieving average gains of 43.4% and 16.0% over the best baseline methods when evaluated with IQL and TD3+BC, respectively. The maximum improvement reaches 57.7% when applying GODA to the Maze2D Large dataset. This highlights GODA’s ability to effectively capture data distributions of various types of datasets and consistently augment high-quality samples.

3) *Adroit tasks.*: Table V presents the normalized scores on Adroit Pena and Door tasks, evaluated using the IQL algorithm, as TD3+BC fails to perform on these tasks. As shown, GODA outperforms all baselines on the Pen-Cloned dataset, although it underperforms on Pen-Human. However, for both datasets in the Door task, GODA demonstrates significant improvements over the best baseline methods. These results further demonstrate that GODA is capable of handling more complex tasks.

B. Extended Experiments on Traffic Signal Control

Table VI presents a comparison of average travel times across different methods for TSC tasks. As shown, while SynthER achieves modest improvements over the performance of models trained on the original datasets, it fails to surpass the original datasets on JN tasks when using the CQL algorithm. In contrast, our GODA consistently outperforms both the original datasets and SynthER across most tasks and all average evaluations. These extended experiments on TSC tasks further validate that GODA is not only applicable to diverse tasks but also capable of improving performance in real-world challenges.

C. Ablation Study

To validate the effectiveness of GODA’s components, we conduct experiments using different configurations.

1) *Ablation on Condition Selection.*: We test three condition selection mechanisms as described in Section IV-B: return-prior, RTG-prior, and random goal conditions. As shown in

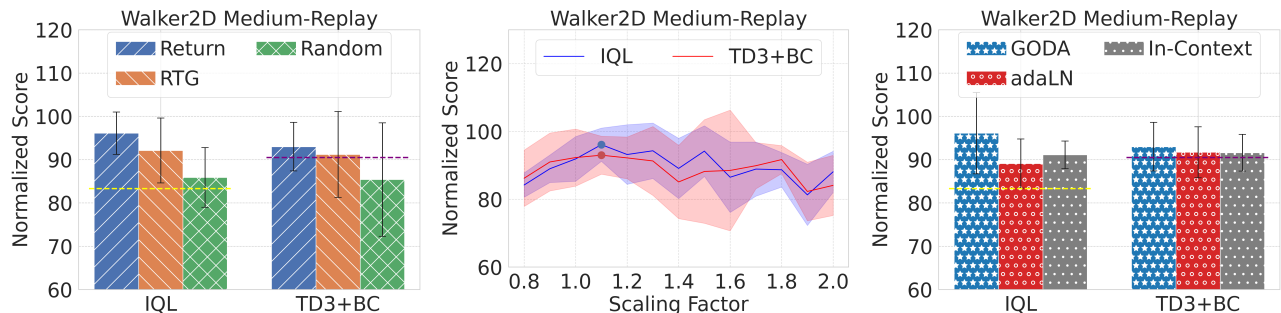


Fig. 6. Ablation studies on condition selection mechanism, goal scaling factor, and adaptive gated conditioning from left to right. Yellow and purple horizon lines represent results for SynthER.

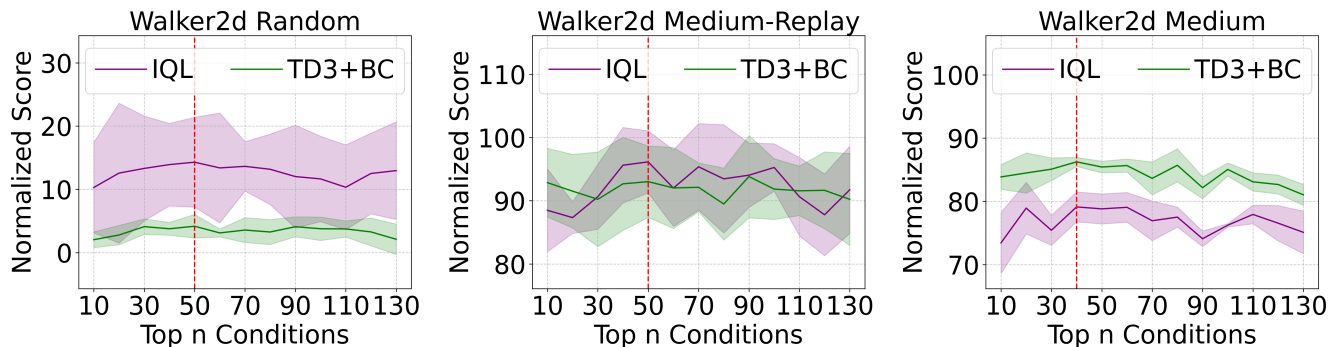


Fig. 7. Ablation study on top n conditions.

the left part of Figure 6, the return-prior method demonstrates superior performance compared to the other two approaches. Moreover, GODA with the return- and RTG-prior conditions outperforms SynthER when tested on two offline RL algorithms. In contrast, the random-prior method shows results comparable to SynthER. This suggests that high-goal conditions identified by the return- and RTG-prior methods enable GODA to generate samples beyond the original data distribution. Randomly selected goal conditions, however, fail to target high-reward regions, producing similar results to SynthER.

2) *Ablation on Goal Scaling Factor:* We further examine the effect of different scaling factors on D4RL tasks, testing values ranging from 0.8 to 2.0. As seen in the middle part of Figure 6, the performance improves as the scaling factor increases but slightly degrades when the scaling factor exceeds 1.1. Scaling factors below 1.0 shrink the selected goals, leading to suboptimal samples. Conversely, scaling factors above 1.1 push the selected goals too far beyond the training data distribution, resulting in diminished performance.

3) *Ablation on Adaptive Gated Conditioning:* Moreover, we evaluate the impact of the adaptive gated conditioning method. We compare GODA with two variants: one using only adaLN conditioning [33], and another using in-context conditioning, where condition embeddings are directly appended to the input embeddings. From the right part of Figure 6, it is clear that GODA with adaptive gated conditioning achieves the best results and the adaLN and in-context conditioning show

similar performance. Additionally, all three methods outperform SynthER which lacks goal conditions. This demonstrates that the inclusion of goal conditions is crucial for guiding the sampling process toward high returns, and our adaptive gated conditioning method enhances the model’s ability to fully utilize these conditions.

4) *Ablation on Top Conditions Selection:* Given that the original datasets contain varying numbers of trajectories, the number of top conditions selected for sampling may differ across datasets. We compare different selections of the top n conditions for each D4RL dataset. Based on the results shown in Figure 7, we empirically select 50 top conditions for the Random and Medium-Replay datasets, and 40 for the Medium datasets.

5) *Ablation on Mixed Datasets:* Since GODA primarily augments samples from high-reward regions of the data distribution, which might result in a lack of diversity, we use a mix of both the original and augmented datasets for training. In this section, we compare the performance of our default setting (mixed datasets) with the use of only augmented datasets. As shown in Figures 8, removing the original datasets leads to slight performance degradation across most tasks. Therefore, combining our augmented datasets with the original datasets helps increase the diversity and extend the reward boundary.

We further present the results for baseline data augmentation methods when combining original datasets with augmented datasets, as shown in Table VII. For Gym tasks, TATU and SynthER exhibit degraded performance when the original

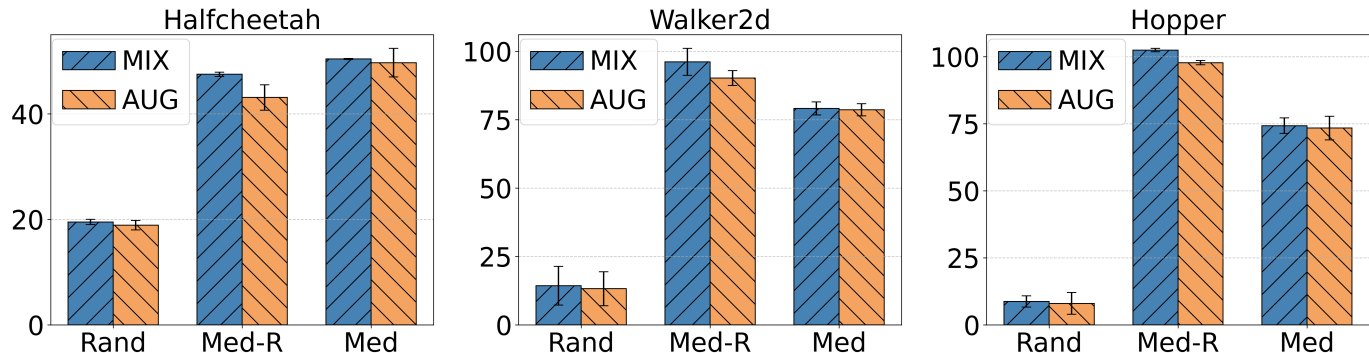


Fig. 8. Ablation on mixed datasets for IQL evaluation.

TABLE VII
DATA QUALITY EVALUATION METRICS FOR SYNTHETIC AND GODA ON WALKER2D TASKS. SMALLER DYNAMICS MSE, LARGER L2 DISTANCE, AND LARGER AVERAGE REWARD INDICATE BETTER QUALITY.

Task	Dataset	IQL				TD3+BC			
		TATU	SynthER	DStitch	GODA	TATU	SynthER	DStitch	GODA
Gym Average	w/o Original Data	46.2±4.3	52.1±2.4	51.5±1.5	52.5±2.9	43.3±4.2	46.3±4.7	47.9±3.3	47.0±4.6
	w/ Original Data	46.0±3.5	51.2±4.4	52.1±1.6	54.7±2.2	41.8±7.9	46.2±4.5	46.8±4.6	48.4±3.9
Maze2D Average	w/o Original Data	45.7±8.2	45.6±2.9	47.5±6.8	66.7±9.3	68.2±10.6	65.1±29.7	65.9±24.9	74.5±11.2
	w/ Original Data	47.1±6.8	44.8±9.2	46.0±8.4	68.1±6.6	68.0±10.9	65.5±37.6	65.1±23.7	79.1±7.5

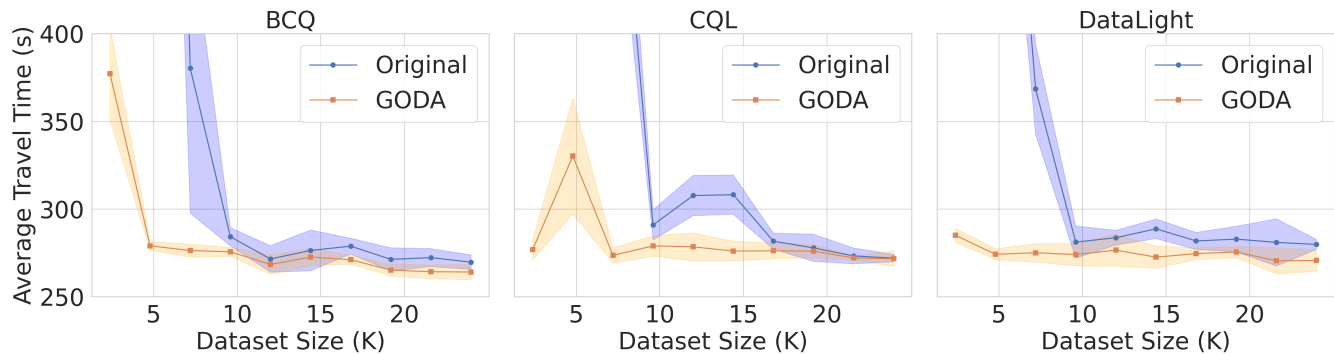


Fig. 9. Performance comparison on JN1 task with different sizes of original real-world training datasets. The parts exceeding the maximum travel time are not displayed.

datasets are included during training, while their performance remains comparable on Maze2D tasks. In contrast, DStitch demonstrates the opposite trend, performing comparably on Gym tasks but worse on Maze2D tasks when using the mixed datasets. Our GODA shows reduced scores when the original datasets are removed; however, its final results remain superior to other baselines. GODA only delivers slightly worse performance than DStitch on Gym tasks when evaluated with TD3+BC but still outperforms TATU and SynthER across all tasks.

6) *Ablation on Size of Original Dataset:* Our experiments on TSC tasks utilize only 24K samples, compared to 1–2M samples for D4RL tasks. The superior performance across both task types demonstrates that GODA not only excels in tasks with large training datasets but also addresses real-world challenges effectively with much smaller datasets. Considering the even greater limitations of original datasets in real-world TSC scenarios, we further evaluate GODA on TSC datasets

with reduced sizes, ranging from 24K to 2.4K samples.

Figure 9 illustrates the performance of different evaluation algorithms trained separately on the original datasets and on the mixture of original and augmented datasets. Notably, we only reduce the size of the original datasets used for directly training the evaluation algorithms or for training GODA, while maintaining the same number of augmented samples (20K) across all cases. Specifically: For the “Original” method, the evaluation algorithms are trained solely on the reduced original datasets. For GODA, the GODA model is first trained on the reduced original datasets, and then 20K augmented samples are generated. The evaluation algorithms are subsequently trained on the mixed datasets.

The results indicate that when the original training datasets contain fewer than 9.6K samples, all three evaluation algorithms trained directly on the reduced original datasets fail to learn effective policies, though their performance improves as the dataset size increases. In contrast, GODA effectively

augments high-quality data, enabling the training of qualified evaluation policies for most sizes of original datasets. Remarkably, GODA achieves this even with only 2.4K samples in the original datasets, failing in just one case each for BCQ and CQL, while consistently demonstrating strong performance otherwise.

VIII. CONCLUSION AND DISCUSSION

This paper proposes a novel goal-conditioned data augmentation method for offline RL, namely GODA, which integrates goal guidance into the data augmentation process. We define the easily obtainable return-to-go signal, along with its corresponding timestep in a trajectory, as the goal condition. To achieve high-return augmentation, we introduce several goal selection mechanisms and a scaling method. Additionally, we propose a novel adaptive gated conditioning structure to better incorporate goal conditions into our diffusion model. We demonstrate that data augmented by GODA shows higher quality than SynthER without goal conditions on different evaluation metrics. Extensive experiments on the D4RL benchmark confirm that GODA enhances the performance of classic offline RL methods when trained on GODA-augmented datasets. Furthermore, we evaluate GODA on real-world traffic signal control tasks. The results demonstrate that GODA is highly applicable to TSC problems, even with very small real-world training datasets, making RL-based methods more practical for real-world applications. In the future, we plan to improve the performance of GODA and explore the application of GODA on more complex real-world challenges.

REFERENCES

- [1] R. S. Sutton and A. G. Barto, *Reinforcement learning: An introduction*. MIT press, 2018.
- [2] C. Bhateja, D. Guo, D. Ghosh, A. Singh, M. Tomar, Q. Vuong, Y. Chebotar, S. Levine, and A. Kumar, “Robotic offline rl from internet videos via value-function learning,” in *2024 IEEE International Conference on Robotics and Automation (ICRA)*. IEEE, 2024, pp. 16 977–16 984.
- [3] S. Guo, L. Zou, H. Chen, B. Qu, H. Chi, S. Y. Philip, and Y. Chang, “Sample efficient offline-to-online reinforcement learning,” *IEEE Transactions on Knowledge and Data Engineering*, 2023.
- [4] G. Li, Y. Shan, Z. Zhu, T. Long, and W. Zhang, “Diffstitch: Boosting offline reinforcement learning with diffusion-based trajectory stitching,” *ICML*, 2024.
- [5] R. Zhang, J. Hou, F. Walter, S. Gu, J. Guan, F. Röhrbein, Y. Du, P. Cai, G. Chen, and A. Knoll, “Multi-agent reinforcement learning for autonomous driving: A survey,” *arXiv preprint arXiv:2408.09675*, 2024.
- [6] L. Zhang and J. Deng, “Data might be enough: Bridge real-world traffic signal control using offline reinforcement learning,” *arXiv preprint arXiv:2303.10828*, 2023.
- [7] X. Du, Z. Li, C. Long, Y. Xing, S. Y. Philip, and H. Chen, “Felight: Fairness-aware traffic signal control via sample-efficient reinforcement learning,” *IEEE Transactions on Knowledge and Data Engineering*, 2024.
- [8] R. F. Prudencio, M. R. Maximo, and E. L. Colombini, “A survey on offline reinforcement learning: Taxonomy, review, and open problems,” *IEEE Transactions on Neural Networks and Learning Systems*, 2023.
- [9] J. Lyu, X. Ma, X. Li, and Z. Lu, “Mildly conservative q-learning for offline reinforcement learning,” *Advances in Neural Information Processing Systems*, vol. 35, pp. 1711–1724, 2022.
- [10] I. Kostrikov, R. Fergus, J. Tompson, and O. Nachum, “Offline reinforcement learning with fisher divergence critic regularization,” in *International Conference on Machine Learning*. PMLR, 2021, pp. 5774–5783.
- [11] J. Zhang, J. Lyu, X. Ma, J. Yan, J. Yang, L. Wan, and X. Li, “Uncertainty-driven trajectory truncation for data augmentation in offline reinforcement learning,” in *ECAI 2023*. IOS Press, 2023, pp. 3018–3025.
- [12] L. Treven, J. Hübötter, F. Dorfler, and A. Krause, “Efficient exploration in continuous-time model-based reinforcement learning,” *Advances in Neural Information Processing Systems*, vol. 36, 2024.
- [13] C. Lu, P. Ball, Y. W. Teh, and J. Parker-Holder, “Synthetic experience replay,” *Advances in Neural Information Processing Systems*, vol. 36, 2024.
- [14] J. Ho, A. Jain, and P. Abbeel, “Denoising diffusion probabilistic models,” *Advances in neural information processing systems*, vol. 33, pp. 6840–6851, 2020.
- [15] T. Karras, M. Aittala, T. Aila, and S. Laine, “Elucidating the design space of diffusion-based generative models,” *Advances in neural information processing systems*, vol. 35, pp. 26 565–26 577, 2022.
- [16] L. Chen, K. Lu, A. Rajeswaran, K. Lee, A. Grover, M. Laskin, P. Abbeel, A. Srinivas, and I. Mordatch, “Decision transformer: Reinforcement learning via sequence modeling,” *Advances in neural information processing systems*, vol. 34, pp. 15 084–15 097, 2021.
- [17] S. Hu, L. Shen, Y. Zhang, and D. Tao, “Prompt-tuning decision transformer with preference ranking,” *arXiv preprint arXiv:2305.09648*, 2023.
- [18] H. Xu, L. Jiang, L. Jianxiong, and X. Zhan, “A policy-guided imitation approach for offline reinforcement learning,” *Advances in Neural Information Processing Systems*, vol. 35, pp. 4085–4098, 2022.
- [19] A. Kumar, J. Fu, M. Soh, G. Tucker, and S. Levine, “Stabilizing off-policy q-learning via bootstrapping error reduction,” *Advances in Neural Information Processing Systems*, vol. 32, 2019.
- [20] T. Yu, A. Kumar, R. Rafailov, A. Rajeswaran, S. Levine, and C. Finn, “Combo: Conservative offline model-based policy optimization,” *Advances in neural information processing systems*, vol. 34, pp. 28 954–28 967, 2021.
- [21] A. Kumar, A. Zhou, G. Tucker, and S. Levine, “Conservative q-learning for offline reinforcement learning,” *Advances in Neural Information Processing Systems*, vol. 33, pp. 1179–1191, 2020.
- [22] Y.-H. Wu, X. Wang, and M. Hamaya, “Elastic decision transformer,” *Advances in Neural Information Processing Systems*, vol. 36, 2024.
- [23] C.-X. Gao, C. Wu, M. Cao, R. Kong, Z. Zhang, and Y. Yu, “Act: Empowering decision transformer with dynamic programming via advantage conditioning,” in *Proceedings of the AAAI Conference on Artificial Intelligence*, vol. 38, no. 11, 2024, pp. 12 127–12 135.
- [24] M. Janner, Y. Du, J. B. Tenenbaum, and S. Levine, “Planning with diffusion for flexible behavior synthesis,” *arXiv preprint arXiv:2205.09991*, 2022.
- [25] C. Chen, F. Deng, K. Kawaguchi, C. Gulcehre, and S. Ahn, “Simple hierarchical planning with diffusion,” *ICLR*, 2024.
- [26] S. Pitis, E. Creager, and A. Garg, “Counterfactual data augmentation using locally factored dynamics,” *Advances in Neural Information Processing Systems*, vol. 33, pp. 3976–3990, 2020.
- [27] N. E. Corrado, Y. Qu, J. U. Balis, A. Labiosa, and J. P. Hanna, “Guided data augmentation for offline reinforcement learning and imitation learning,” *arXiv preprint arXiv:2310.18247*, 2024.
- [28] J. Sohl-Dickstein, E. Weiss, N. Maheswaranathan, and S. Ganguli, “Deep unsupervised learning using nonequilibrium thermodynamics,” in *International conference on machine learning*. PMLR, 2015, pp. 2256–2265.
- [29] Y. Song, J. Sohl-Dickstein, D. P. Kingma, A. Kumar, S. Ermon, and B. Poole, “Score-based generative modeling through stochastic differential equations,” *arXiv preprint arXiv:2011.13456*, 2020.
- [30] A. Rahimi and B. Recht, “Random features for large-scale kernel machines,” *Advances in neural information processing systems*, vol. 20, 2007.
- [31] A. Vaswani, N. Shazeer, N. Parmar, J. Uszkoreit, L. Jones, A. N. Gomez, Ł. Kaiser, and I. Polosukhin, “Attention is all you need,” *Advances in neural information processing systems*, vol. 30, 2017.
- [32] O. Ronneberger, P. Fischer, and T. Brox, “U-net: Convolutional networks for biomedical image segmentation,” in *Medical image computing and computer-assisted intervention—MICCAI 2015: 18th international conference, Munich, Germany, October 5–9, 2015, proceedings, part III 18*. Springer, 2015, pp. 234–241.
- [33] W. Peebles and S. Xie, “Scalable diffusion models with transformers,” in *Proceedings of the IEEE/CVF International Conference on Computer Vision*, 2023, pp. 4195–4205.
- [34] K. He, X. Zhang, S. Ren, and J. Sun, “Deep residual learning for image recognition,” in *Proceedings of the IEEE conference on computer vision and pattern recognition*, 2016, pp. 770–778.
- [35] S. Elfwing, E. Uchibe, and K. Doya, “Sigmoid-weighted linear units for neural network function approximation in reinforcement learning,” *Neural networks*, vol. 107, pp. 3–11, 2018.

- [36] U. M. Ascher and L. R. Petzold, *Computer methods for ordinary differential equations and differential-algebraic equations*. SIAM, 1998.
- [37] J. Fu, A. Kumar, O. Nachum, G. Tucker, and S. Levine, “D4rl: Datasets for deep data-driven reinforcement learning,” *arXiv preprint arXiv:2004.07219*, 2020.
- [38] A. Rajeswaran, V. Kumar, A. Gupta, G. Vezzani, J. Schulman, E. Todorov, and S. Levine, “Learning complex dexterous manipulation with deep reinforcement learning and demonstrations,” *arXiv preprint arXiv:1709.10087*, 2017.
- [39] H. Zhang, S. Feng, C. Liu, Y. Ding, Y. Zhu, Z. Zhou, W. Zhang, Y. Yu, H. Jin, and Z. Li, “Cityflow: A multi-agent reinforcement learning environment for large scale city traffic scenario,” in *The world wide web conference*, 2019, pp. 3620–3624.
- [40] L. Zhang, Q. Wu, J. Shen, L. Lü, B. Du, and J. Wu, “Expression might be enough: representing pressure and demand for reinforcement learning based traffic signal control,” in *International Conference on Machine Learning*. PMLR, 2022, pp. 26 645–26 654.
- [41] S. Fujimoto and S. S. Gu, “A minimalist approach to offline reinforcement learning,” *Advances in neural information processing systems*, vol. 34, pp. 20 132–20 145, 2021.
- [42] S. Fujimoto, D. Meger, and D. Precup, “Off-policy deep reinforcement learning without exploration,” in *International conference on machine learning*. PMLR, 2019, pp. 2052–2062.
- [43] D. Tarasov, A. Nikulin, D. Akimov, V. Kurenkov, and S. Kolesnikov, “Corl: Research-oriented deep offline reinforcement learning library,” *Advances in Neural Information Processing Systems*, vol. 36, 2024.